QuickField Analysis of a Three-Phase Encapsulated Busbars System

Ioan Popa[*] , Marian Ciontu[*] , Alin-Iulian Dolan[*]

[*] University of Craiova/Faculty of Electrical Engineering, Craiova, Romania, ipopa@elth.ucv.ro
[*] University of Craiova/Faculty of Electrical Engineering, Craiova, Romania, mciontu@elth.ucv.ro
[*] University of Craiova/Faculty of Electrical Engineering, Craiova, Romania, adolan@elth.ucv.ro

***Abstract* - In this paper, we propose an approach for the magnetic and thermal analysis of a three-phase encapsulated busbars system for high currents using QuickField software. This paper proposes a numerical model developed by coupling of the magnetic field problem with the stationary heat field problem for the geometry of a single-phase execution busbars system. The coupling of problems is realized by importing specific losses from the magnetic field problem as heat sources for thermal field problem. The magnetic field problem is also coupled to the electrical circuit. The shields are short-circuited at both ends and they are connected to the ground. For this constructive solution, in the shields occur induced currents, approximately equals to those of conductors. The analyzed constructive solution has two conductors in parallel per phase, by technological reasons, and therefore electrodynamic forces appear between them. Due to the shielding effect, the magnetic field is practically zero outside of shield and therefore the forces do not occur between phases. In the model it was taken into account the variation of electrical conductivity with the temperature. The thermal model has been validated by an analytical procedure for calculating the active conductor and shield temperatures. The global coefficient of heat transfer by convection and radiation used in thermal model was estimated using the power losses computed by magnetic model. There is a good agreement between analytically calculated temperatures and those numerically calculated. The presented model can be used for analysis, design and optimization of three-phase busbars systems in single phase execution.**

Keywords - *encapsulated busbars, high currents, AC magnetics model, steady-state heat transfer model, coupled problems*

I. Introduction

The shielded busbars systems are used to establish the connection between the generator and the transformer in a power plant. There are two types of construction [1], [2]:

- Single phase execution with short-circuited shields at both ends and connected to ground (Fig. 1) or with interrupted by segments shield and connected to ground;

- Three-phase execution, with a common grounded shield.

For the single phase execution, the active conductor (of aluminum) is placed in a metal grounded shield (also of aluminum). For the three-phase execution all the active conductors are arranged in a common grounded shield.

Internal insulation (between the active conductor and the shield) is performed in air at normal pressure or with SF_6 gas at a pressure of 3-5 bars.

The construction of shielded busbars must meet the following requirements:

- The elimination of the ability to produce accidental short circuits (insulation pollution etc.).

- The elimination of the possibility of accidental electrocution by touching the bars under tension;

- The low annual costs (return of investments and the Joule losses in the shields);

- Reduction of electrodynamics forces.

If the shields are short-circuited and grounded at both ends then they produce a circulation of currents ($\underline{I}_{1e} = -\underline{I}_{1c}, \underline{I}_{2e} = -\underline{I}_{2c}, \underline{I}_{3e} = -\underline{I}_{3c}$, Fig. 1) approximately equals and in opposite phase with corresponding currents of active conductors. This construction involves a close to zero magnetic field outside the shield and therefore the electrodynamics forces acting between phases are close to zero. This is one of the advantages of this technical solution, but a disadvantage is represented by the Joule losses in the shield.

In the case of single phase execution with interrupted shield but grounded, the electrodynamics forces have great values and their calculation is based on the following observations:

1) The magnetic field produced by the current of active conductor is not affected by the concentric shield.

2) The magnetic field produced by the current of the active conductor is strongly attenuated by a neighboring shield.

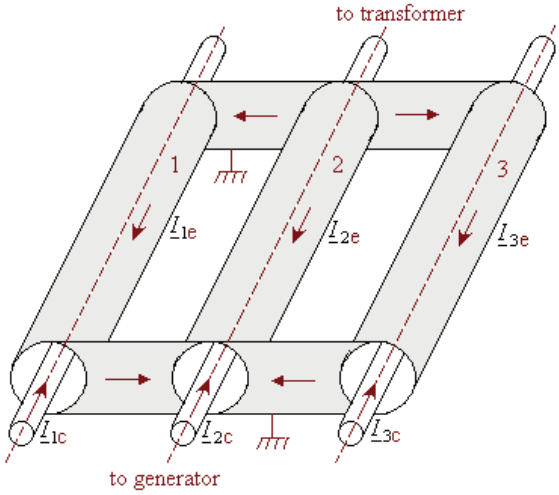

Fig. 1. Three phase busbars system with short-circuited shields at both ends

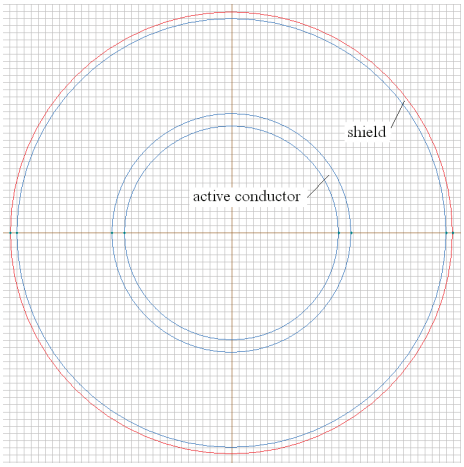

Fig. 2. Geometry of a hollow cylindrical conductor for single phase

In the paper the execution of single-phase busbars is analyzed.

II. 2-D Numerical Models

The numerical analysis in QuickField [8] is based on coupling of magnetic field problem (created in AC Magnetics module) with the thermal field problem (created in Steady-state heat transfer module).

The purpose of numerical analysis is to determine:
- losses by Joule effect in shields and active conductors in rated and short-circuit regimes;
- electrodynamics forces in steady-state and short-circuit regime, acting on both conductors of each phase.

A. AC MagnetAC Magnetic model

The numerical model is an AC magnetic problem coupled with the electric circuit. The fundamental equation of the magnetic field [3], [4], [5], [6] using finite elements method, written in terms of the magnetic vector potential $\vec{A}$ is

$$\nabla \times \left(\frac{1}{\mu} \nabla \times \vec{A} \right) - \sigma \frac{\partial \vec{A}}{\partial t} = -\vec{J}_0 \cdot \qquad (1)$$

where $\vec{J}_0$ is the applied source current density, μ is the permeability and σ is the electric conductivity.

The problem of magnetic field was coupled with electric circuit (Fig. 7) and the boundary conditions are Neumann type ($\vec{A} = 0$).

B. Electric circuit model coupled to magnetic field model

The electric circuit created in QuickField is shown in Fig. 3 containing the current sources I_1, I_2, I_3 , two active conductors per phase and three corresponded shields. Short-circuiting and grounding shields at both ends are simulated in the circuit by grounding resistance $R = 8\ \Omega$.

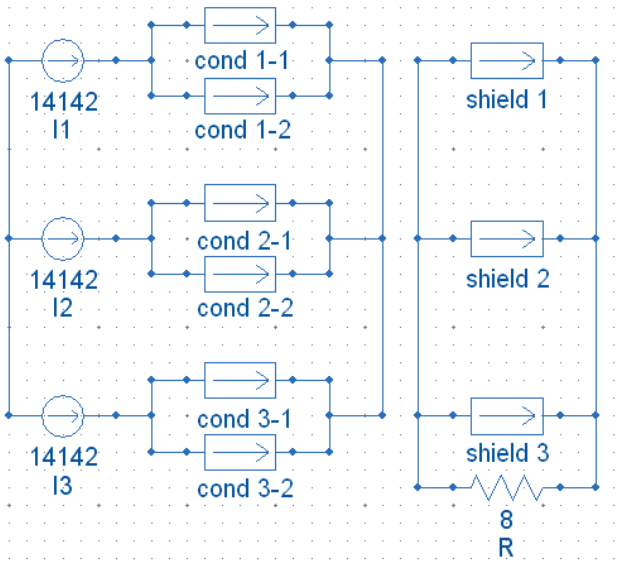

Fig. 3. Electric circuit model coupled to magnetic field model.

C. Steady-state thermal model

The thermal field is described by the equation

$$\frac{\partial}{\partial x}\left(\lambda \frac{\partial T}{\partial x} \right) + \frac{\partial}{\partial y}\left(\lambda \frac{\partial T}{\partial y} \right) + S(T) = 0 \cdot \qquad (2)$$

where λ is the thermal conductivity, T - the temperature and S – source term (Joule losses in active conductor and shield).

The boundary conditions are Dirichlet type on boundary of the magnetic model (ambient temperature) and heat convection type on the exterior and interior surfaces of conductors and shields.

The principle of thermal model is based on the following physical phenomena [1], [2] (Fig. 3):

- in active conductors the heat flux P_1 by Joule and skin effects is generated and it is sent to the shield by convection and conduction ways (P_{1c} through thermal resistance R_{t1c}) and radiation way (P_{1r} through thermal resistance R_{t1r});
- in the shield, the heat flux P_2 by eddy currents and / or circulating currents is generated, together with heat flow P_1 and transmitted to the environment by convection and conduction ways (P_{1c} + P_{2c} through thermal resistance R_{t2c}) and radiation way (P_{1r} + P_{2r} through thermal resistance R_{t2r});

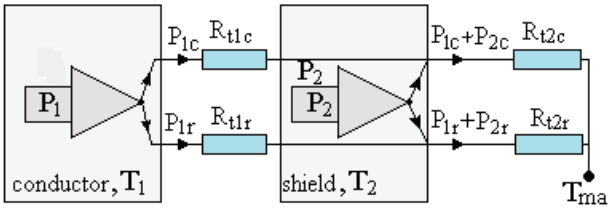

Fig. 4. The principle of thermal model (T_1 - conductor temperature, T_2 - shield temperature, T_{ma} - ambient temperature).

D. Shield temperature

The global thermal transmissivity can be calculated with relationship

$$\alpha = M\left(T_2 - T_{ma}\right)^{0.2}. \tag{3}$$

where:

$$M = 2.65K_B\varepsilon T_{ma}^3 + 0.9\left(\frac{\lambda^4 c_p \rho^2 \beta g}{\mu d_c^2}\right)^{0.2}. \tag{4}$$

where K_B – Boltzmann constant, ε - shield emissivity, λ - air thermal conductivity, c_p – air specific heat capacity, ρ - air density, β - volumetric expansion coefficient, g - gravitational acceleration, μ - dynamic viscosity, d_c – characteristic dimension (exterior shield diameter).

The thermal flux transmitted to the environment by shield surface unity is

$$P_e = \frac{P_1 + P_2}{A} = \frac{P_1 + P_2}{\pi D} = \alpha \Delta T. \tag{5}$$

where A is exterior surface shield area per length unity, D is exterior shield diameter and $\Delta T = T_2 - T_{ma}$.

From (3) and (5) results the relationship for global thermal transmissivity

$$\alpha = \left(M P_e^{\,0.2}\right)^{1/1.2}. \tag{6}$$

The overtemperature of the shield will be

$$\Delta T = \frac{P_e}{\alpha}. \tag{7}$$

and shield temperature

$$T_2 = T_{ma} + \Delta T. \tag{8}$$

E. Conductor temperature

To determine the active conductor temperature is calculated both heat flux transferred by conduction and convection and heat flux transferred by radiation.

The heat flux transferred by convection and conduction from the active conductor to shield is approximated by the relationship [2]

$$P_{1c} = \left(T_1 - T_2\right)^{1.2} \cdot 2\pi\lambda \cdot 0.4\left(\frac{\rho(r_2 - r_1)^3}{\mu}\mathrm{Pr}\right)^{0.2} \cdot \frac{1}{\ln\left(\frac{r_2}{r_1}\right)} \tag{9}$$

where r_1 - exterior radius of active conductor, r_2 - interior radius of the shield and the parameters λ, ρ, μ and Pr (Prandtl number) concerns the gas between active conductor and shield. The difference $r_2 - r_1$ is considered the characteristic dimension.

The relationship (9) can be written

$$P_{1c} = b\left(T_1 - T_2\right)^{1.2} \tag{10}$$

where

$$b = 2\pi\lambda \cdot 0.4\left(\frac{\rho(r_2 - r_1)^3}{\mu}\mathrm{Pr}\right)^{0.2} \cdot \frac{1}{\ln\left(\frac{r_2}{r_1}\right)} \tag{11}$$

The thermal flux transferred by radiation from active conductor to shield is calculated by relationship

$$P_{1r} = c\left(T_1^4 - T_2^4\right) \tag{12}$$

where

$$c = \frac{2\pi r_1 K_B}{\frac{1}{\varepsilon_1} + \left(\frac{1}{\varepsilon_2} - 1\right)\frac{r_1}{r_2}} \tag{13}$$

Adding the two thermal flux, from (10) and (12) results the equation

$$b(T_1 - T_2)^{1.2} + c(T_1^4 - T_2^4) = P_1, \tag{14}$$

where the coefficients b and c are known (from (11) and (13)) and T_2 is absolute shield temperature and it is known. The total thermal flux P_1 is computed by AC Magnetic model (see table 1).

The equation (14) is iteratively solved and results the active conductor temperature T_1.

F. Analytical results

With the next values of quantities in equations (3) – (14) $\theta_{ma} = 40^{\circ}\mathrm{C}$, $\lambda = 0.027\ \mathrm{W/(m \cdot K)}$, $\varepsilon = 0.61$, $c_p = 1010\ \mathrm{J/(kg \cdot K)}$, $\rho = 1.128\ \mathrm{kg/m^3}$, $\beta = 0.003194$, $d_c = 0.97\ \mathrm{m}$, $P_1 \cong P_2 = 205\ \mathrm{W/m}$, $\varepsilon_1 = 0.9$, $\varepsilon_2 = 0.9$, $r_1 = 0.216\ \mathrm{m}$, $r_2 = 0.48\ \mathrm{m}$, $\mathrm{P_r} = 0.713$, it results the global heat transfer coefficient $\alpha = 7\ \mathrm{W/(m^2K)}$, shield temperature $\theta_2 = 59^{\circ}\mathrm{C}$ and active conductor temperature $\theta_1 = 77.43^{\circ}\mathrm{C}$.

In previous thermal analytical computation model it was considered a hollow cylindrical conductor with the same cross-section area to the geometry model in Fig. 3.

III. Numerical Results and Discussions

In developing numerical models it was used the geometry of the encapsulated busbar system in single-phase execution, in a power plant from Romania (Fig. 5) having U_n = 24 kV, I_n = 10 kA, I_t = 125 kA, t = 1s, $i_d = 300\ \mathrm{kA}$ (peak value).

In the last time, the technological solution with the hollow cylindrical conductor (Fig. 2) is also used, which has the advantage that the electrodynamic force acting on the active conductor is zero.

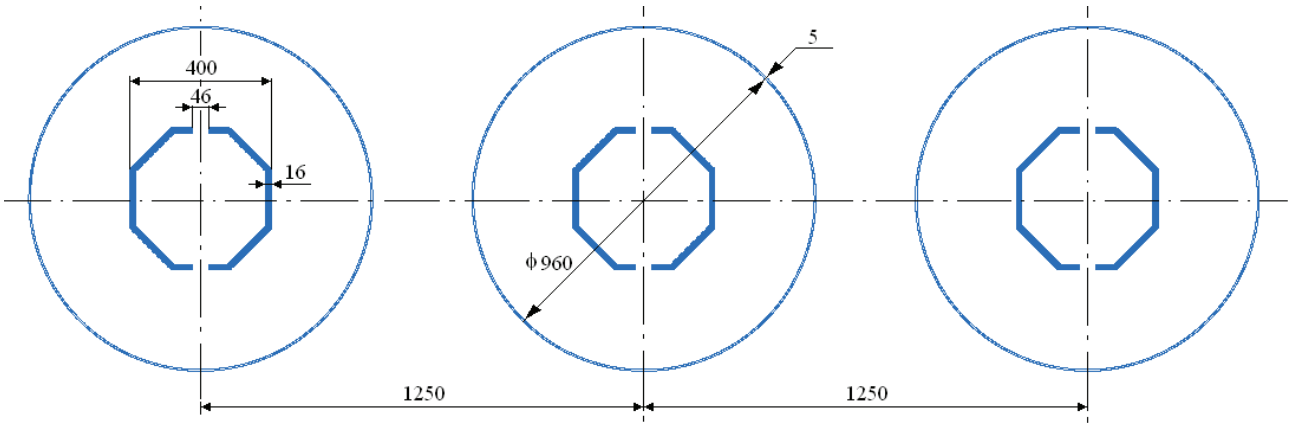

Fig. 5. System geometry.

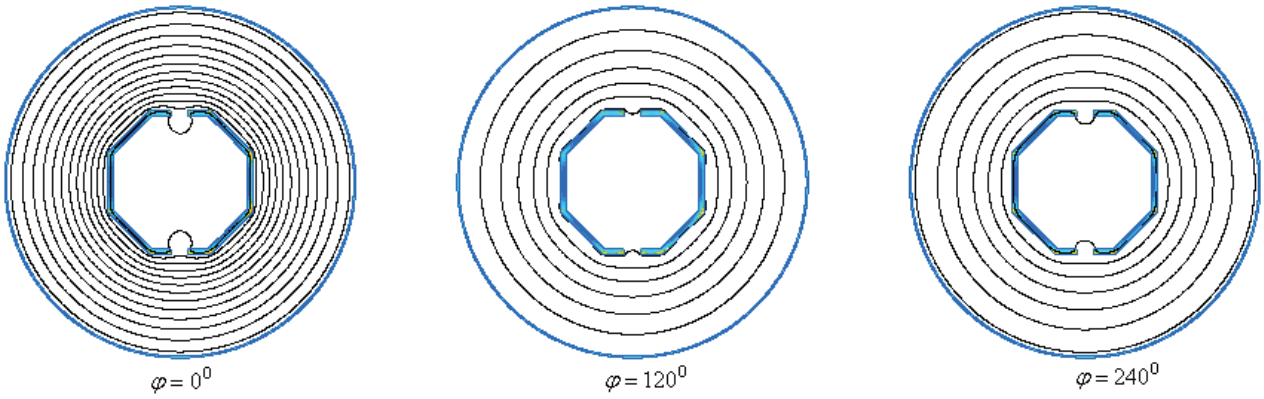

Fig. 6. Magnetic flux density lines (shield effect).

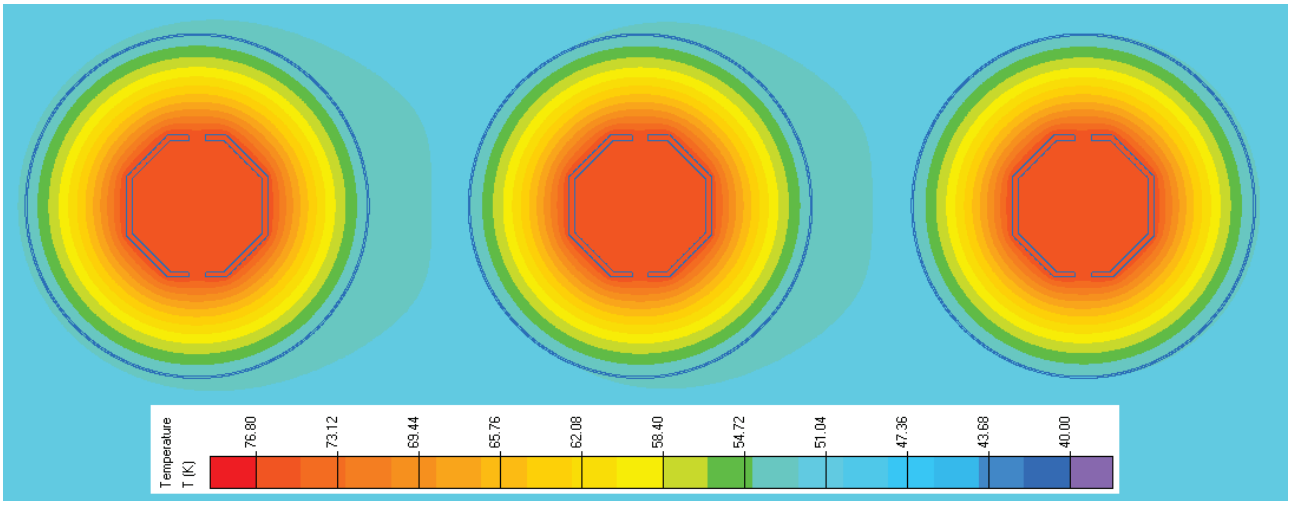

Fig. 7. Thermal field distribution.

TABLE I. PHYSICAL QUANTITIES IN BUSBARS SYSTEM AT RATED CURRENT (I_n = 10 kA, RMS value)

	Conductor 1	Conductor 2	Conductor 3	Shield 1	Shield 2	Shield 3
Joule heat [W/m]	203.95	203.96	203.95	208.58	203.58	198.39
Total current (peak value) [A]	14142	14142	14142	14324	14147	13968
Total inductance [H/m]	$3.542 \cdot 10^{-7}$	$3.511 \cdot 10^{-7}$	$3.472 \cdot 10^{-7}$			
Impedance [Ω/m]	$2.222 \cdot 10^{-4}$	$2.210 \cdot 10^{-4}$	$2.193 \cdot 10^{-4}$			

Resistance [Ω/m]	$1.562 \cdot 10^{-5}$	$1.799 \cdot 10^{-5}$	$1.529 \cdot 10^{-5}$			
Reactance [Ω/m]	$2.216 \cdot 10^{-4}$	$2.203 \cdot 10^{-4}$	$2.187 \cdot 10^{-4}$			
Voltage drop [mV/m]	785.57	781.33	775.20	5.97	5.97	5.97
	Cond. 1-1	Cond. 1-2	Cond. 2-1	Cond. 2-2	Cond. 3-1	Cond. 3-2
Maxwell force (average value) [N/m]	14.009	-13.966	13.967	-13.972	13.962	-13.996
Maxwell force (oscillating component) [N/m]	13.994	13.953	13.953	13.958	13.945	13.982

TABLE II. PHYSICAL QUANTITIES IN BUSBARS SYSTEM AT SHORT-TIME RATING CURRENT (I_n = 125 kA, RMS value)

	Conductor 1	Conductor 2	Conductor 3	Shield 1	Shield 2	Shield 3
Joule heat [W/m]	7966.8	7967.2	7966.8	8082.8	7890.8	7691
Total current (peak value) [A]	88387.5	88387.5	88387.5	89516	88425	87310
Total inductance [H/m]	$3.542 \cdot 10^{-7}$	$3.511 \cdot 10^{-7}$	$3.472 \cdot 10^{-7}$			
Impedance [Ω/m]	$2.222 \cdot 10^{-4}$	$2.210 \cdot 10^{-4}$	$2.193 \cdot 10^{-4}$			
Resistance [Ω/m]	$1.562 \cdot 10^{-5}$	$1.799 \cdot 10^{-5}$	$1.529 \cdot 10^{-5}$			
Reactance [Ω/m]	$2.216 \cdot 10^{-4}$	$2.203 \cdot 10^{-4}$	$2.187 \cdot 10^{-4}$			
Voltage drop [V/m]	4.9094	4.883	4.845	0.037	0.037	0.037
	Cond. 1-1	Cond. 1-2	Cond. 2-1	Cond. 2-2	Cond. 3-1	Cond. 3-2
Maxwell force (average value) [N/m]	547.21	-545.58	545.59	-545.8	545.39	-546.69
Maxwell force (oscillating component) [N/m]	546.62	545.06	545.03	545.22	544.73	545.15

TABLE III. PHYSICAL QUANTITIES IN BUSBARS SYSTEM AT CURRENT SHOCK (I_n = 300 kA, peak value)

	Conductor 1	Conductor 2	Conductor 3	Shield 1	Shield 2	Shield 3
Joule heat [W/m]	7966.8	7967.2	7966.8	93115	90903	88602
Total current (peak value) [A]	300000	300000	300000	303830	301130	296340
	Cond. 1-1	Cond. 1-2	Cond. 2-1	Cond. 2-2	Cond. 3-1	Cond. 3-2
Maxwell force (average value) [N/m]	6403.9	-6285.2	6285.3	-6287.8	6283	-6298
Maxwell force (oscillating component) [N/m]	6297.1	6279.2	6278.3	6281.1	6275.4	6291.7

A. Numerical results

The figure 6 shows the distribution of magnetic flux density for the busbars system geometry in Fig. 4, for the three phases with specified phase angles. Note the shielding effect caused by eddy currents. In out-side of shield, a 15-20 times decreases of magnetic flux density is obtained (reduction factor) compared to inner-side of the shield (d-e zone in Fig. 10).

The figure 8 presents the distribution of current density in one of two conductors per phase of analyzed busbars system geometry. In this case it can be seen an uneven distribution of current density on thickness and also along the side of the octagon conductor, with a concentration around the exterior octagon coins.

In Fig. 9 is done the variation of the current density versus shield radius.

In Fig. 10 is shown the variation of magnetic flux density for phase 2 (median), on the horizontal symmetry axis. Note that out-side of shield, the magnetic flux density strongly decreases (e-f zone, Fig. 10).

Figure 7 shows the distribution of thermal field in the system busbars. In the thermal model, heat sources (Joule heat) in conductors and shield are imported from magnetic model.

Since in the magnetic model the electrical conductivity is temperature dependent, between the two coupled problems have made several iterations to correlate its value to the temperature resulting from the thermal model.

On the conductor and shield heat transfer surfaces it was used a global heat transfer coefficient by convection and radiation resulting from equation (6), but ambient temperature for different heat transfer surfaces was obtained by attempts, such that the numerical computed conductor temperature to be equal to that analytical obtained (equation 14). The comparative values are presented in Table IV.

In Tables I, II and III are summarized the physical quantities obtained with the numerical model developed in QuickField, in rated and short circuit regimes.

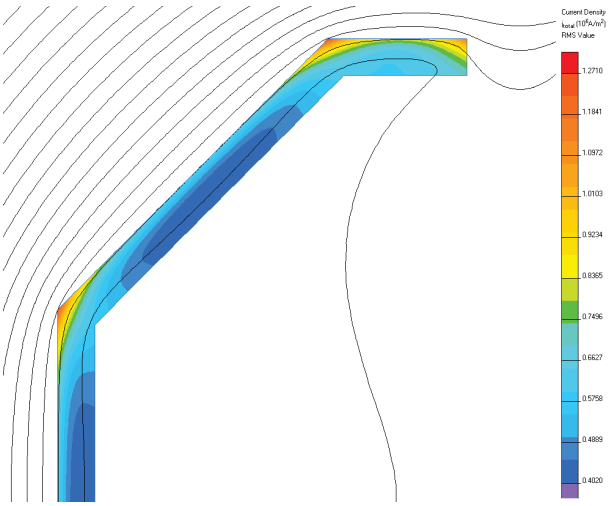

Fig. 8. Current density distribution in active conductor - detail.

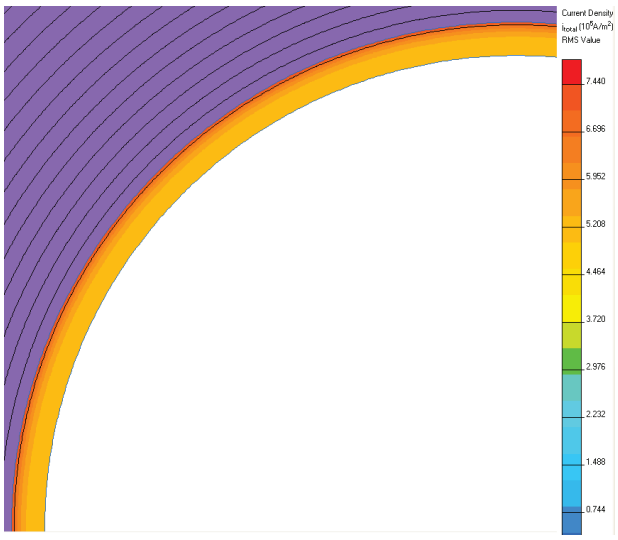

Fig. 11. Current density distribution for a hollow cylindrical conductor .

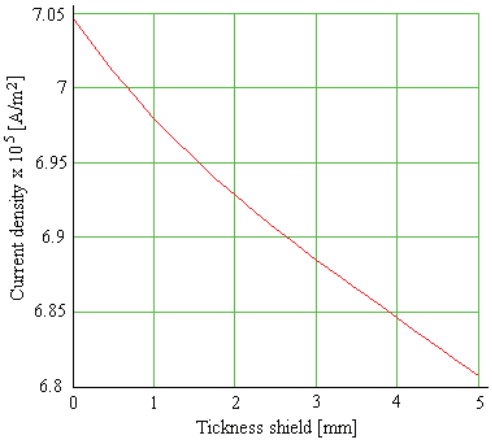

Fig. 9 Current density in shield.

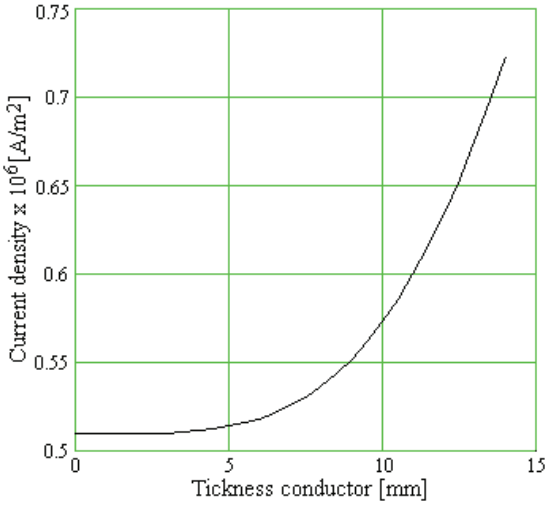

Fig. 12. Current density variation for a hollow cylindrical conductor .

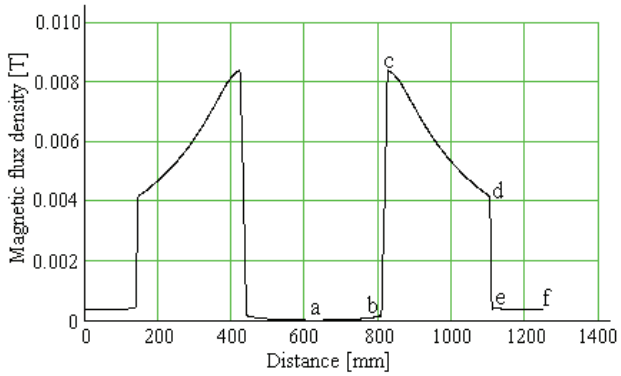

Fig. 10. Magnetic flux density variation (a-b – interior of conductor, b-c – in conductor, c-d – beetwen conductor and shield, d-e – in shield, e-f – outside shield).

TABLE IV. TEMPERATURES IN CONDUCTOR AND SHIELD

Temperature	Analytical	QuickField
Conductor, θ_1 [^{o}C]	77.43	76.6
Shield, θ_2 [^{o}C]	59	54.06

IV. CONCLUSIONS

The numerical model developed in QuickField software, in rated and short-circuit regimes, allows the following facilities:

- determination of the losses in conductors and shields (by Joule effect and eddy currents);
- determination of the electrodynamic forces acting between the conductors of the same phase, being practically zero between the conductors of different phases, due to the shielding effect;
- determination of the temperature distribution in busbar system in single-phase execution;
- determination of physical quantities such as ohmic resistance in a.c., impedance, inductance and impedance of each conductor, magnetic energy, voltage drop etc.

The numerical model can be used to optimize the construction of busbars system. Also, the model can be used to determine the maximum temperature in short-circuit

regime if the problem in steady-state heat transfer is coupled to the problem of transient heat transfer. The analysis of non-stationary short-circuit thermal regime is not the subject of this paper.

The numerical model can be used to design and optimize the geometry of three-phase busbars system in single phase execution and it has been analytically validated for the thermal field problem.

REFERENCES

[1] Gh. Hortopan, "Aparate electrice de comutație, vol 1 – Principii (in roumanian)," Editura Tehnică, Bucureşti, 2000.

[2] Gh. Hortopan, I.O. Vlase, S. Nițu, "Ecranarea electromagnetică în tehnica curenților intenşi (in roumanian)", Editura Tehnică, Bucureşti, 1990.

[3] M. De Wulf, P. Wouters, P. Sergeant, L. Dupré, E. Hoferlin, S. Jacobs, P. Harlet, "Electromagnetic shielding of high-voltage cable," *Journal of Magnetism and Magnetic Materials.,*316(2007) e908 – e911, 2007.

[4] V. Hatziathanassiou, D. Labridis, "Coupled magneto-thermal field computation in three-phase gas insulated cables," *Archiv fur Elektrotechnik – Part 1:Finite element formulation,".,*76(1993), 285-292, 1993.

[5] E. Salinas, "Conductive and ferromagnetic screening of 50 Hz magnetic field from a three-phase system of busbars," *Journal of Magnetism and Magnetic Materials",* 226 – 230, 1239 – 1241, 2001.

[6] K. C. Agrawal, "Electrical Power Engineering – Reference & Applications Handbook" Copyrighted Material, 2007.

[7] D. Meeker, *Finite element method magnetics, version 4.2,* http://www.femm.info/wiki/HomePage, 2012.

[8] Tera Analysis Ltd., *QuickField Software version 5.10 Professional,* http://quickfield.com, 2013.